Engineered neural tissue with aligned, differentiated adipose-derived stem cells promotes peripheral nerve regeneration across a critical sized defect in rat sciatic nerve

Melanie Georgiou [a, b], Jon P. Golding [b], Alison J. Loughlin [b], Paul J. Kingham [c, 1], James B. Phillips [b, d, *, 1]

[a] Advanced Centre for Biochemical Engineering, Bernard Katz Building, University College London, Gordon Street, London WC1H 0AH, UK
[b] Department of Life Health & Chemical Sciences, The Open University, Walton Hall, Milton Keynes MK7 6AA, UK
[c] Department of Integrative Medical Biology, Umeå University, SE 901 87 Umeå, Sweden
[d] Biomaterials & Tissue Engineering, UCL Eastman Dental Institute, University College London, 256 Gray's Inn Road, London WC1X 8LD, UK

ARTICLE INFO

ABSTRACT

Adipose-derived stem cells were isolated from rats and differentiated to a Schwann cell-like phenotype *in vitro*. The differentiated cells (dADSCs) underwent self-alignment in a tethered type-1 collagen gel, followed by stabilisation to generate engineered neural tissue (EngNT-dADSC). The pro-regenerative phenotype of dADSCs was enhanced by this process, and the columns of aligned dADSCs in the aligned collagen matrix supported and guided neurite extension *in vitro*. EngNT-dADSC sheets were rolled to form peripheral nerve repair constructs that were implanted within NeuraWrap conduits to bridge a 15 mm gap in rat sciatic nerve. After 8 weeks regeneration was assessed using immunofluorescence imaging and transmission electron microscopy and compared to empty conduit and nerve graft controls. The proportion of axons detected in the distal stump was 3.5 fold greater in constructs containing EngNT-dADSC than empty tube controls. Our novel combination of technologies that can organise autologous therapeutic cells within an artificial tissue construct provides a promising new cellular biomaterial for peripheral nerve repair.

© 2014 The Authors. Published by Elsevier Ltd. This is an open access article under the CC BY license (http://creativecommons.org/licenses/by/3.0/).

1. Introduction

Peripheral nerve injuries lead to pain and significant disability in many affected individuals. Each year approximately 300,000 people of working age in Europe experience a peripheral nerve injury (PNI) [1]; of these less than 50% regain full function after treatment [2,3]. For peripheral nerve damage that results in gaps greater than approximately 3 cm, the current clinical gold standard treatment is the nerve autograft. Many new therapeutic strategies for improving nerve repair are being developed in basic, pre-clinical and clinical trials. Results have shown that guidance conduit structures and living cells are essential for the repair of larger nerve gaps to provide trophic support and recreate the environment provided by the nerve autograft [4–9].

Among the strategies being developed for peripheral nerve repair, the combination of tissue engineering and stem cell technologies represents a powerful approach for generating artificial nerve tissue that could be used in the clinical setting. We recently developed effective technology for the production of engineered neural tissue (EngNT), an aligned cellular biomaterial for nerve repair [10]. The technology involved Schwann cell self-alignment within a tethered collagen hydrogel, followed by a stabilisation process to form robust, aligned cellular sheets. EngNT containing aligned Schwann cells was used within a nerve repair conduit to promote neuronal regeneration across a critical sized defect in the rat sciatic nerve [10]. This approach differs from other tissue engineering approaches because the cells and the extracellular matrix align as a consequence of integrin-mediated cell-generated forces acting within a constrained hydrogel environment [11]. The result is an artificial tissue containing aligned Schwann cells distributed evenly throughout an aligned collagen hydrogel matrix. A key factor limiting the translation of this and other cellular tissue-

* Corresponding author. Department of Biomaterials & Tissue Engineering, UCL Eastman Dental Institute, 256 Gray's Inn Road, London WC1X 8LD, UK. Tel.: +44 020 3456 1254.
E-mail address: jb.phillips@ucl.ac.uk (J.B. Phillips).
[1] Joint senior authors.

engineered constructs towards clinical application is the source of Schwann cells. Autologous human Schwann cells would need to be derived from invasive nerve biopsies and sufficient cell numbers for regeneration would only become available after a lengthy expansion time *in vitro* [12]. Schwann cell-like cells derived from stem cells are therefore a more attractive source because they can potentially be obtained from the patient for use in an autologous therapy [13]. Autologous cells are generally considered to be more readily accepted by the patient because they do not provoke an immune reaction [7,14].

Adipose-derived stem cells (ADSCs) are an accessible source of adult stem cells that have generated considerable interest as candidates for autologous cell transplantation and they are currently being used in clinical trials for a wide range of indications. Stem and progenitor cells usually make up less than 5% of the total cell population in adipose tissue [15], but this is 2500-fold more than the frequency of such cells in bone marrow [16]. The abundance of ADSCs and the ability to collect large amounts of adipose tissue via liposuction potentially eliminates the need for cell expansion. They are easily accessible in large quantities with little donor site morbidity or patient discomfort. Experimental studies using rat ADSCs have shown that these cells have the ability to differentiate along the glial lineage, making them good potential candidates for use as an alternative to Schwann cells in peripheral nerve repair [17—20]. Rat ADSCs differentiated into Schwann cell-like cells (dADSCs) express a range of Schwann cell proteins, they can promote neurite outgrowth *in vitro* [17—20] and enhance regeneration *in vivo* [21—24]. The regenerative properties of these cells has been attributed to their secretion of neurotrophic factors [25,26], their ability to recruit host Schwann cells to aid the regenerative process [27], their possible direct contribution to myelin formation [24] and their ability to enhance the survival of sensory and motor neurons [28]. Importantly, recent studies indicate that human ADSCs, stimulated by the same protocol as used in the rodent experiments, also have a pro-regenerative phenotype when transplanted into the injured peripheral nervous system [29,30].

The aforementioned studies have used a variety of different types of conduits to deliver the dADSCs to the injury site. Cells have been transplanted in fast resorbing fibrin conduits [21,22,29], synthetic nerve tube conduits [28,31] or naturally occurring decellularised matrices [32]. The aim of this study was to test for the first time whether dADSCs can be used to generate EngNT through cellular self-alignment followed by stabilisation within collagen gels, avoiding the need for construction of aligned scaffolds and subsequent seeding of cells that is common in other tissue engineering approaches [11]. Following characterisation of dADSC morphology and phenotype in EngNT *in vitro*, EngNT-dADSC constructs were tested in a critical sized defect in the rat sciatic nerve that simulates the clinical long gap injury scenario in order to assess their ability to support neuronal growth *in vivo*.

2. Materials and methods

All experimental procedures involving animals were conducted in accordance with the UK Animals (Scientific Procedures) Act (1986)/the European Communities Council Directives (86/609/EEC) and approved by the Open University Animal Ethics Advisory Group and the Northern Swedish Committee for Ethics in Animal Experiments.

2.1. Isolation, culture and differentiation of adipose-derived stem cells

Fat tissue was harvested from adult rats and the ADSCs were isolated as previously described [19]. Cells were cultured in modified Eagle's medium (α-MEM; Invitrogen, UK) containing 10% (v/v) foetal bovine serum (FBS) and 1% (v/v) penicillin/streptomycin solution. The cultures were maintained at sub-confluent levels in a 37 °C incubator with 5% CO₂ and passaged with trypsin/EDTA (Invitrogen, UK) when required. The multi-potent potential of the cell cultures was assessed by ensuring their ability to differentiate along several lineages, as described previously [19]. To differentiate the adipose stem cells into a Schwann cell-like phenotype

(dADSCs), growth medium was removed from sub-confluent cultures at passage 2 and replaced with medium supplemented with 1 mM β-mercaptoethanol (Sigma––Aldrich, UK) for 24 h. Then the cells were washed and fresh medium supplemented with 35 ng/ml all-trans-retinoic acid (Sigma) was added. A further 72 h later, the cells were washed and the medium was replaced with differentiation medium containing cell growth medium supplemented with 14 μM forskolin (Sigma), 10 ng/ml basic fibroblast growth factor (bFGF; Pepro Tech Ltd., UK), 5 ng/ml platelet-derived growth factor (PDGF-AA; Pepro Tech Ltd., UK) and 252 ng/ml neuregulin NRG1 (R&D Systems, UK). The cells were incubated for a minimum 2 weeks under these conditions with fresh medium added approximately every 72 h.

2.2. Immunofluorescence staining of dADSCs

Cells were seeded at a density of 10,000 cells/well in an 8-well LabTek chamber slide and allowed to settle for 48 h before they were fixed for 20 min in 4% (w/v) paraformaldehyde at room temperature. The cells were then washed in phosphate buffered saline (PBS) before the addition of 5% (v/v) normal goat serum (NGS) and 5% (v/v) normal horse serum (NHS) together with 0.1% Triton X-100 (v/v) in PBS for a further 15 min at room temperature. The blocking serum was then removed and the primary antibodies, mouse monoclonal anti-GFAP (Millipore) and rabbit polyclonal anti-S100B (Dako) at respective dilutions of 1:500 and 1:1000 were added and the samples incubated overnight at 4 °C. The cells were then washed in PBS, re-blocked using NGS and NHS before addition of the secondary antibodies, Alexa 350 conjugated goat anti-rabbit IgG (1:50 dilution) and Alexa 488 conjugated goat anti-mouse IgG (1:300 dilution) for 2 h at room temperature. The samples were then washed 3 × 15 min with PBS before repeating the blocking step with NGS and NHS. Mouse monoclonal anti-p75NTR (Abcam, dilution 1:500) was then added and incubated overnight at 4 °C. The cells were then washed in PBS, 3 × 15 min, before a final blocking step in NGS and NHS. Finally the secondary antibody Alexa 568 conjugated goat anti-mouse IgG (1:300 dilution) was added for 2 h at room temperature before final washes with PBS and addition of ProlongGold anti-fade mountant. Images were captured at 200× final magnification using a Nikon Eclipse 90i microscope with a Nikon DS-U2 digital camera. Five random images were recorded from each well and a total of 4 wells for each preparation were imaged. dADSCs were analysed from 2 different rats and these were then used for further *in vitro* studies and parallel *in vivo* transplantations.

2.3. Fabrication of EngNT-dADSC

EngNT was prepared according to methods described previously [10]. dADSCs were maintained in Dulbecco's Modified Eagle's Medium (DMEM; Gibco) supplemented with penicillin and streptomycin (100 U/ml and 100 mg/ml, respectively; Sigma), 10% (v/v) FBS and the growth factors used for differentiation as described above. To prepare gels, 1 volume of 10× Minimum Essential Medium (Sigma) was mixed with 8 volumes of type I rat tail collagen (2 mg/ml in 0.6% acetic acid; First Link, UK) and the mixture neutralised using sodium hydroxide before addition of 1 volume of dADSCs suspension (final density 4 × 10⁶ cells per ml of gel). One ml of this mixture was added to each mould at 4 °C and integrated with tethering mesh at opposite ends before setting at 37 °C for 10 min. Tethered gels were immersed in culture medium and incubated at 37 °C in a humidified incubator with 5% CO₂/95% air for 24 h during which time the cells aligned. Aligned cellular gels were stabilised by plastic compression: gels were separated from the tethering mesh using a scalpel, placed on an absorbent paper pad and immediately compressed by loading the gel with 120 g for 1 min during which time fluid was absorbed by the paper pad underneath [33]. The resulting sheets of EngNT were either transferred directly to 24-well plates for *in vitro* experiments, or rolled to form rods (approximately 200 μm diameter × 15 mm length) and maintained in culture medium for up to 24 h prior to *in vivo* experiments.

2.4. RT-PCR of cultured dADSCs and EngNT-dADSC

Total RNA was isolated from the samples using an RNeasy™ kit (Qiagen) and one step RT-PCR (Qiagen) was performed using 1 ng of RNA per reaction mix. The samples were loaded into a thermocycler (Biometra, Germany) which was used with the following parameters: a reverse transcription (RT) step (50 °C, 30 min) and a nucleic acid denaturation/RT inactivation step (95 °C, 15 min) followed by 28—34 cycles of denaturation (95 °C, 30 sec), annealing (30 sec) and primer extension (72 °C, 1 min) followed by a final extension incubation (72 °C, 5 min). Forward and reverse primer (all 5′ → 3′) pairs for a variety of glial cell markers and neurotrophic factors were manufactured by SigmaAldrich and are listed in Table 1 together with their annealing temperatures. The reaction product amplicons were electrophoresed at 50 V for 90 min through a 1.5% (w/v) agarose gel and their size was estimated using Hyperladder IV (Bioline, UK). Samples were visualised under ultraviolet (UV) illumination following GelRed™ nucleic acid stain (Bio Nuclear, Sweden) incorporation into the agarose.

2.5. Assessment of EngNT-dADSC in co-culture with neurons

Dissociated dorsal root ganglion (DRG) neurons were prepared from adult (200—300 g) Sprague Dawley rats. DRGs were incubated in collagenase (0.125%; Sigma) for 1.5 h at 37 °C then dissociated by trituration and washed twice with 20 ml

Table 1
Primer sequences for RT-PCR and annealing temperatures used (°C).

Gene	Forward primer (5′ → 3′)	Reverse primer (5′ → 3′)	°C
S100B	GTTGCCCTCATTGATGTCTTC	AGACGAAGGCCATAAACTCCT	57.9
GFAP	GCTGAACTGAACCAGCTTCGA	CTTGGCCACATCCATCTCCAC	57.3
P75	GAGCCGTGCAAGCCGTGCAAC	CTCAGGCTCCTGGGTGCTGGG	64
P0	GGTGGTGCTGTTGCTGCTG	TTCGTGCTTCGGCTGTGGTC	68.0
NGF	AAGGATCCTGGACCCAAGCTCACCTCA	GAGTGACGTGGATGAGCGCTTGCTCCT	67.0
BDNF	ATGGGACTCTGGAGAGCGTGAA	CGCCAGCCAATTCTCTTTTTGC	65.3
GDNF	TCACCAGATAAACAAGCGGC	TACATCCACACCGTTTAGCG	61.0
VEGF-A	TGCACCCACGACAGAAGGGGA	TCACCGCCTTGGCTTGTCACA	60.0
18S	TCAACTTTCGATGGTAGTCGC	CCTCCAATGGATCCTCGTTAA	62.1

of culture medium before being incubated for 18 h with cytosine arabinoside (0.01 mM) to deplete glia. The resulting cultures with a purity of >99% neurons were seeded onto the surface of EngNT-dADSC sheets, allowed to settle for 30 min, then constructs were immersed in culture medium at 37 °C in a humidified incubator with 5% CO_2/95% air. After 3 days the co-cultures were washed briefly in PBS and fixed in 4% (w/v) paraformaldehyde at 4 °C for 24 h, then immunofluorescence staining was carried out as described previously for collagen gels [34,35] to detect βIII-tubulin positive neurons and S100B positive dADSCs.

Confocal microscopy (Leica SP5) was used to assess the neurite alignment in the EngNT-dADSC-neuron co-cultures. Six equivalent fields were analysed per gel using a standardised sampling protocol. Images were captured using a ×40 oil immersion lens, z-stacks were 20 μm with a step size of 1 μm. Image analysis was conducted using Volocity™ software (Perkin Elmer, Waltham, MA) running automated 3D image analysis protocols to measure the angle of dADSC alignment and of neurite alignment compared to the long axis of the construct.

2.6. Surgical repair of rat sciatic nerve

Sprague Dawley (250—500 g) rats were deeply anesthetised by inhalation of isoflurane, the left sciatic nerve of each animal was exposed at mid-thigh level, transected and then either a repair conduit or a nerve graft was positioned between the stumps to produce an inter-stump distance of 15 mm. Conduits or grafts were retained in place using three 10/0 epineurial sutures at each stump, then wounds were closed in layers and animals were allowed to recover for 8 weeks. Neuronal regeneration was assessed across a 15 mm inter-stump distance and included three groups (7 rats in each): (A) empty NeuraWrap™ conduit, (B) two EngNT-dADSC rods in a NeuraWrap™ sheath (18 mm long) or (C) a 15 mm nerve graft taken from a littermate culled using CO_2 asphyxiation. Animals were culled following the recovery period using CO_2 asphyxiation and repaired nerves were excised under a dissecting microscope. The middle of the repair device was removed and prepared for transmission electron microscopy (TEM), and transverse cryostat sections (10 μm thick) were prepared from the proximal and distal parts of the device and the nerve stumps. The transverse sections that were used for analysis were from positions 1 mm into the proximal and distal stumps, or 1 mm into the proximal and distal parts of the repair site, measured from the end of the nerve stump in each case.

Sections were blocked using 5% horse serum for 20 min then immunostained using mouse monoclonal anti-200 kDa neurofilament to detect axons (1:1000, Covance, Princeton, NJ) and visualised with DyLight 549 horse anti-mouse immunoglobulin secondary antibody (1:200, Vector Laboratories, Burlingame,
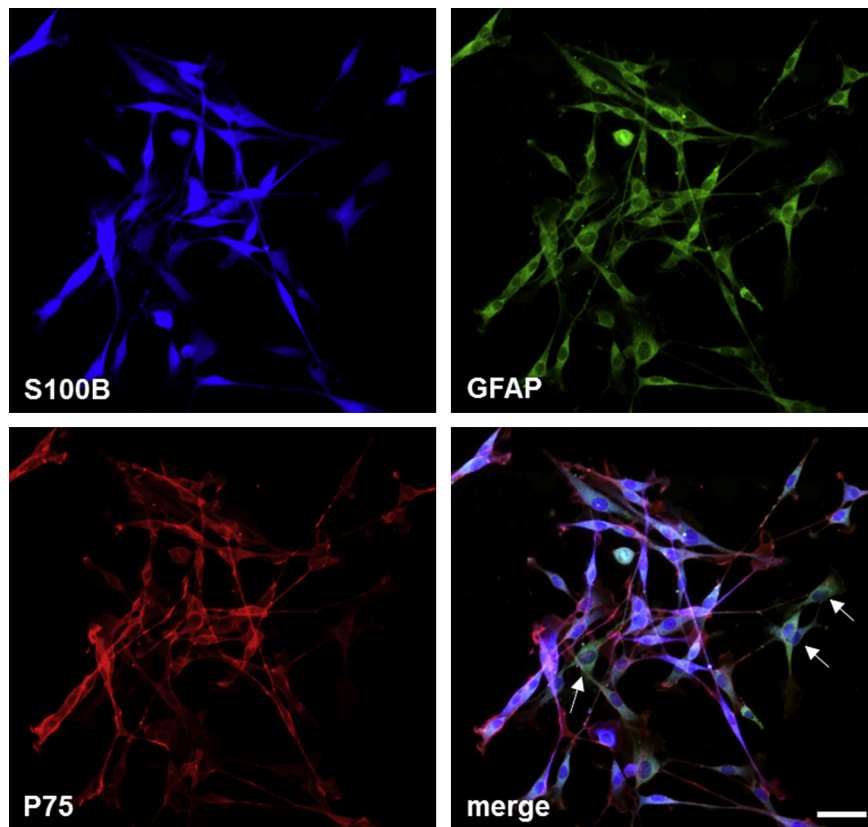

Fig. 1. Characterisation of transplanted cells. Adipose tissue derived stem cells were treated with a mixture of glial growth factors as described in the Materials and Methods. Immunostaining for S100B, GFAP, and P75 showed the majority of the cells expressed all 3 Schwann cell markers, the remaining cells were predominantly S100B and GFAP double positive (arrows). Scale bar = 25 μm.
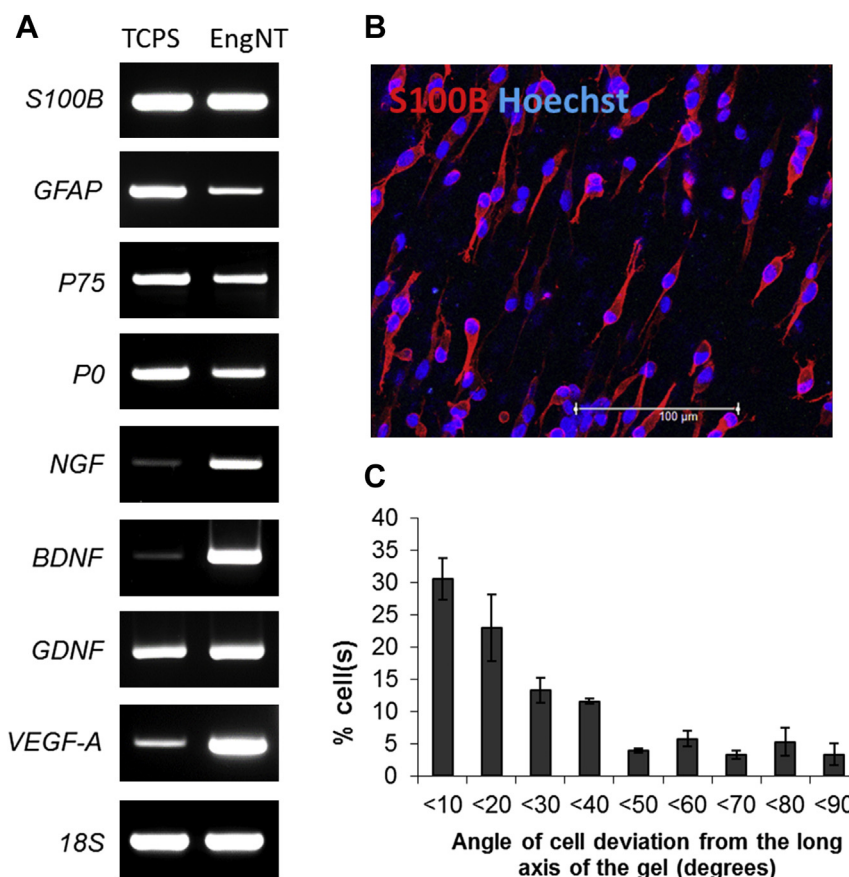
Fig. 2. Characterisation and alignment of Schwann cell-like cells (dADSC) within engineered neural tissue (EngNT). (A) RT-PCR showing the expression of Schwann cell molecules and growth factors expressed by dADSCs cultured on tissue culture plastic substrate (TCPS) and within EngNT. 18S was used as a house-keeping control gene. (B) Confocal micrographs show highly aligned and elongated cells labelled with S100B. Z-distance 20 μm, step size 1 μm, scale bars are 100 μm. (C) Image analyses indicated that the cells were predominantly aligned with the long axis of the material. Data are mean frequency of angle deviation (in 10° bins) ± SEM from 3 fields in each construct, $n = 3$ independent gels.

CA). Primary antibody was incubated overnight at 4 °C and secondary antibody was incubated at room temperature for 45 min. Sections were mounted using VECTASHIELD mounting medium (Vector Laboratories, Peterborough, UK) and fluorescence microscopy (Olympus BX61) was used to quantify axonal growth by counting all of the neurofilament positive axons present in each transverse section.

2.7. TEM

After excision and dissection of the middle of the repair constructs, samples were fixed in 4% (w/v) paraformaldehyde in PBS for 24 h at 4 °C. These were post-fixed in 1% (w/v) osmium tetroxide in PBS, dehydrated through a graded series of acetone, flat-embedded in Epon epoxy resin and polymerized at 60 °C for 48 h. Semi-thin sections of 1 μm were cut using a glass knife on a UCT ultra microtome (Leica, UK), dried onto poly-L-lysine coated microscope slides and stained with 1% (w/v) toluidine blue with added 5% (w/v) sodium borate. Ultrathin sections of 70 nm were cut with a diamond knife (Diatome, UK) and collected on copper slot grids with Pioloform/carbon support films. Sections were counter-stained with aqueous uranyl acetate and Reynolds' lead citrate before examination in a JEM 1400 TEM (JEOL, UK). Ultrathin sections were imaged at a column magnification of ×2000 from the areas of greatest regeneration density as identified from the respective stained semi-thin sections. These images were coded for subsequent analyses, and Image J software was used to measure axon and fibre diameter, myelin thickness and G-ratio were calculated where appropriate.

2.8. Statistical analysis

Normality of data was tested using a Kolmogorov–Smirnov normality test prior to using either one-way or repeated measures ANOVA where appropriate. Where ANOVA showed a statistically significant result ($P < 0.05$), a Tukey's post-test was performed to compare all pairs of groups and the P values from the post-test are indicated on the figures.

3. Results

3.1. Characterisation and testing of EngNT-dADSC in vitro

Rat adipose-derived stem cells were differentiated to a Schwann cell-like phenotype (dADSCs) as previously described [19]. After two weeks *in vitro* differentiation, 81.88 ± 4.69% of the dADSCs showed positive immunoreactivity for the Schwann cell markers S100B, GFAP and P75 (Fig. 1). Preliminary studies determined the optimum cell-seeding density for dADSCs to align within tethered collagen gels within 24 h (4×10^6 cells/ml) and confirmed that the cells survived the stabilisation process (cell viability was 99.5 ± 0.86% (mean ± SEM, $n = 4$) assessed using propidium iodide exclusion). The pattern of gene expression for key markers of the Schwann cell lineage was compared in dADSCs growing on tissue culture polystyrene and in EngNT (Fig. 2A). RT-PCR analysis showed that cells growing in the EngNT also expressed a wide range of neurotrophic factors (Fig. 2A). Confocal microscopy showed that the EngNT contained elongated dADSCs exhibiting a bipolar morphology (Fig. 2B) and orientated parallel to the long axis of the material, with over 65% of the cells showing a deviation of less than 30° from the long axis (Fig. 2C).

To determine the ability of the EngNT-dADSCs to support and guide neuronal growth, primary rat DRG neurons were seeded onto the surface of the aligned cellular sheets and maintained in culture for 3 days. Long neurites were detected growing in close contact with the columns of aligned dADSCs in the material (Fig. 3A). The 3-dimensional orientation of the neurites corresponded closely to the
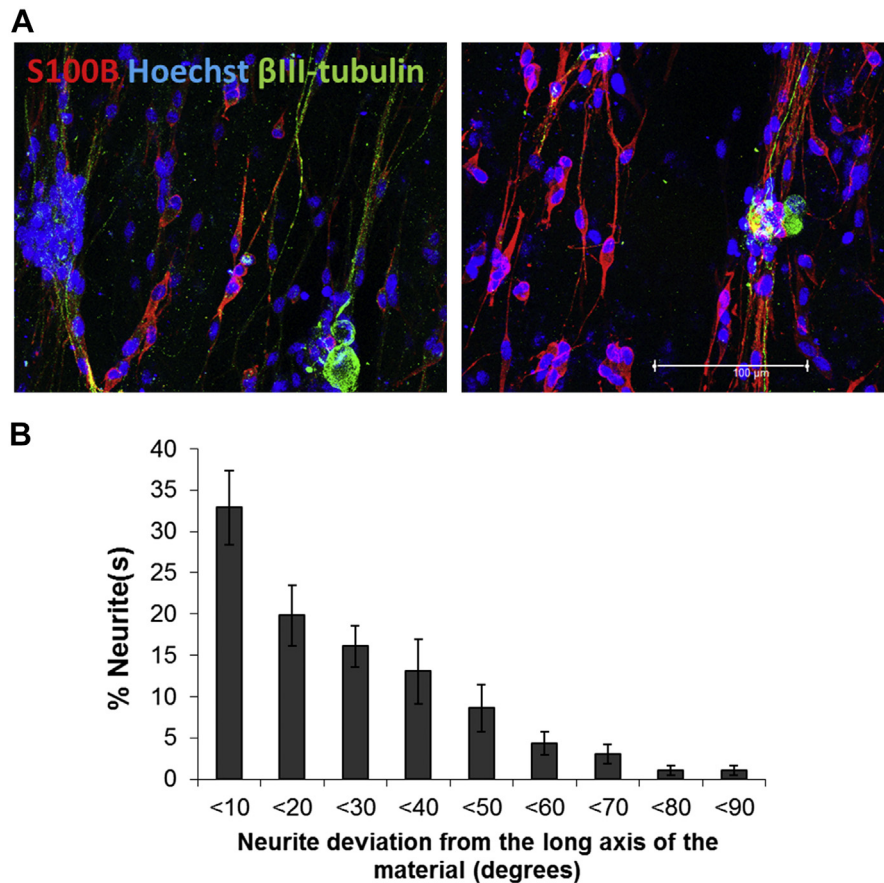
Fig. 3. EngNT-ADSC supports and guides neuronal growth *in vitro*. (A) Confocal micrographs show the dADSC (red) supporting aligned neurite growth (green) after 3 days in co-culture (z-dimension 20 μm, step size 1 μm, scale bars are 100 μm). (B) Three-dimensional image analysis was used to quantify the neuronal growth from 6 fields in each construct (the total length of extended neurites in the sampled area was 9447 ± 1710 μm, mean ± SEM, and the total area sampled per construct was 0.736 μm^2). The angle of neurite growth was compared to the long axis of the material and revealed that the neurite growth was mainly parallel to the long axis of the material, which also corresponds to the direction of dADSC alignment. (For interpretation of the references to colour in this figure legend, the reader is referred to the web version of this article.)

direction of dADSC alignment, with 69% of neurites showing a deviation of less than 30° from the long axis of the gel (Fig. 3B).

3.2. EngNT-dADSC supports neuronal regeneration in vivo

EngNT-dADSC sheets were rolled to form rods, then two rods were ensheathed within a NeuraWrap™ conduit to form an implantable device. EngNT-dADSC conduits were tested in a 15 mm gap in the rat sciatic nerve over an 8 week recovery period and compared to empty NeuraWrap or nerve graft controls. Toluidine blue stained semi-thin sections from the middle of the repairs showed that regenerated neural tissue was present throughout the nerve graft and EngNT-dADSC samples with sparse smaller patches present in the empty tube controls (Fig. 4A). The areas of highest density were selected for TEM (Fig. 4B) and the diameter of nerve fibres and the extent of myelination assessed (Supplementary Fig. 1). Myelin thickness was significantly lower in the empty tube controls compared to the nerve graft group, whereas there was no significant difference in myelin thickness between the EngNT-dADSC group and the nerve graft group. There were no significant differences in axon diameter, fibre diameter or G-ratio between the three experimental groups.

Detailed analyses were conducted using immunohistochemistry in multiple locations within the repaired nerve tissue (proximal stump, PS; proximal part of the device, PD; distal part of the device, DD; distal stump, DS) to investigate neuronal regeneration (Fig. 5A

and B). All three groups showed similar numbers of axons in the proximal stumps, with half the number of axons present in the proximal part of the empty tube controls compared to the nerve graft group (Fig. 6A). In the distal part of the repairs and the distal stumps there was minimal regeneration through the empty tube controls, confirming that this rat model mimics the poor regeneration seen in critical size 'long-gap' repairs in humans. The EngNT-dADSC conduits supported 3.5-fold more regenerating axons than the empty tube controls in both the DD and DS, although this was significantly fewer than in the nerve graft controls (Fig. 6A). To normalise for the differences in growth of neurons into the different repair constructs and facilitate comparisons, the number of axons in the distal regions was expressed as a percentage of the number of axons detected in the proximal part of the repair in each case (Fig. 6B).

4. Discussion

Here we report the formation of EngNT using dADSCs, the characterisation of dADSC phenotype within EngNT, and the ability of EngNT-dADSC to support and guide neurite regeneration *in vitro*. When implanted within a critical-sized defect in the rat sciatic nerve, EngNT-dADSC supported robust neural regeneration across the gap and into the distal stump. The combination of dADSCs with the EngNT assembly technique provides a promising method for building replacement peripheral nerve tissue using autologous cells.
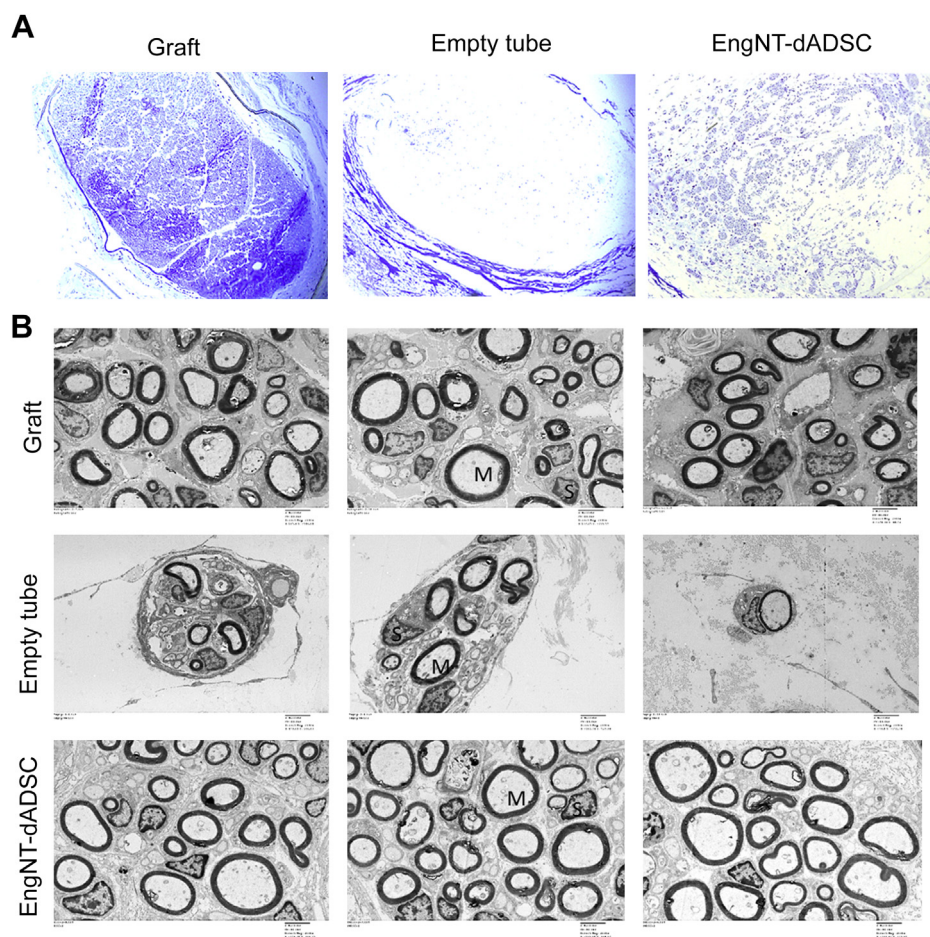
Fig. 4. EngNT-dADSC supports neuronal regeneration in a long gap rat sciatic nerve injury model. (A) Representative semi-thin sections stained with toluidine blue were taken from the mid-point of the conduits or grafts 8 weeks following nerve repair (×20 magnification). (B) The areas with the highest density were sampled and imaged with TEM (*M* = myelinated axon, *S* = Schwann cell nucleus, scale bar 2 μm). (For interpretation of the references to colour in this figure legend, the reader is referred to the web version of this article.)

We characterised the dADSCs under regular tissue culture conditions and after they had been transplanted and aligned in the collagen gels. Consistent with previous studies the dADSCs expressed a range of Schwann cell markers and neurotrophic factors [19,28]. Importantly the expression of these markers was maintained in the gels. The differentiation process used to generate the dADSCs has been shown to enhance the ability of the cells to evoke *in vitro* neurite outgrowth [17,19] and this has been attributed to elevated levels of NGF and BDNF [18]. Stimulation of human cells also increases the expression of NGF, BDNF and GDNF [29,30]. Furthermore, the cells cultured in the collagen gels showed enhanced levels of growth factor mRNAs compared to those cultured on tissue culture plastic. This might be a consequence of placing the cells in 3D or of specific cell-ECM interactions within the gels. For example, previously it was shown that the ECM molecules fibronectin and laminin can activate the dADSC to a more neurotrophic phenotype, although no changes in specific growth factor expression levels could be detected [36]. Interestingly there was an indication that the expression of GFAP may have decreased when dADSCs were incorporated in the EngNT, which is consistent with our previous data comparing astrocyte GFAP expression in monolayer and 3D cell culture [34].

Morphologically the dADSCs adopted an aligned elongated shape in the tethered collagen gels that persisted in the EngNT and was reminiscent of the Schwann cells in the Bands of Büngner [37].

The effectiveness of EngNT-dADSC to support and guide regeneration of DRG neurons was demonstrated using a co-culture model in which regenerating neurites appeared to grow along the chains of aligned dADSCs. This is in line with our previous work using other cells in EngNT [10,38] and previous reports from others that used cell level topography and Schwann cell-neuron contact to direct neuronal growth [39–41]. Three-dimensional quantification of the angle of neurite orientation confirmed that the EngNT-dADSC guided regeneration along the long axis of the cellular material. This type of anisotropy is a critical feature in the design of nerve repair materials [5], where the support of robust neuronal regeneration must also be directed efficiently across the gap to facilitate rapid recovery.

Given the positive results obtained using EngNT-dADSC *in vitro* we proceeded to investigate the effects *in vivo*. Rat dADSCs have previously been shown to boost the rate of early axon regeneration and enhance sensory neuron survival in a rat sciatic nerve injury model [22,28]. Stimulated human adipose stem cells also enhance the *in vivo* expression levels of regeneration associated genes [29]. The mechanism of the action of the stem cells has not been definitively elucidated but some studies suggest that they work by either releasing growth factors themselves [42] or by modulating the endogenous Schwann cells [27]. Magnetic resonance imaging (MRI) has also confirmed the effects of ADSCs on the early histological measurements of axon regeneration. Tremp et al. were able
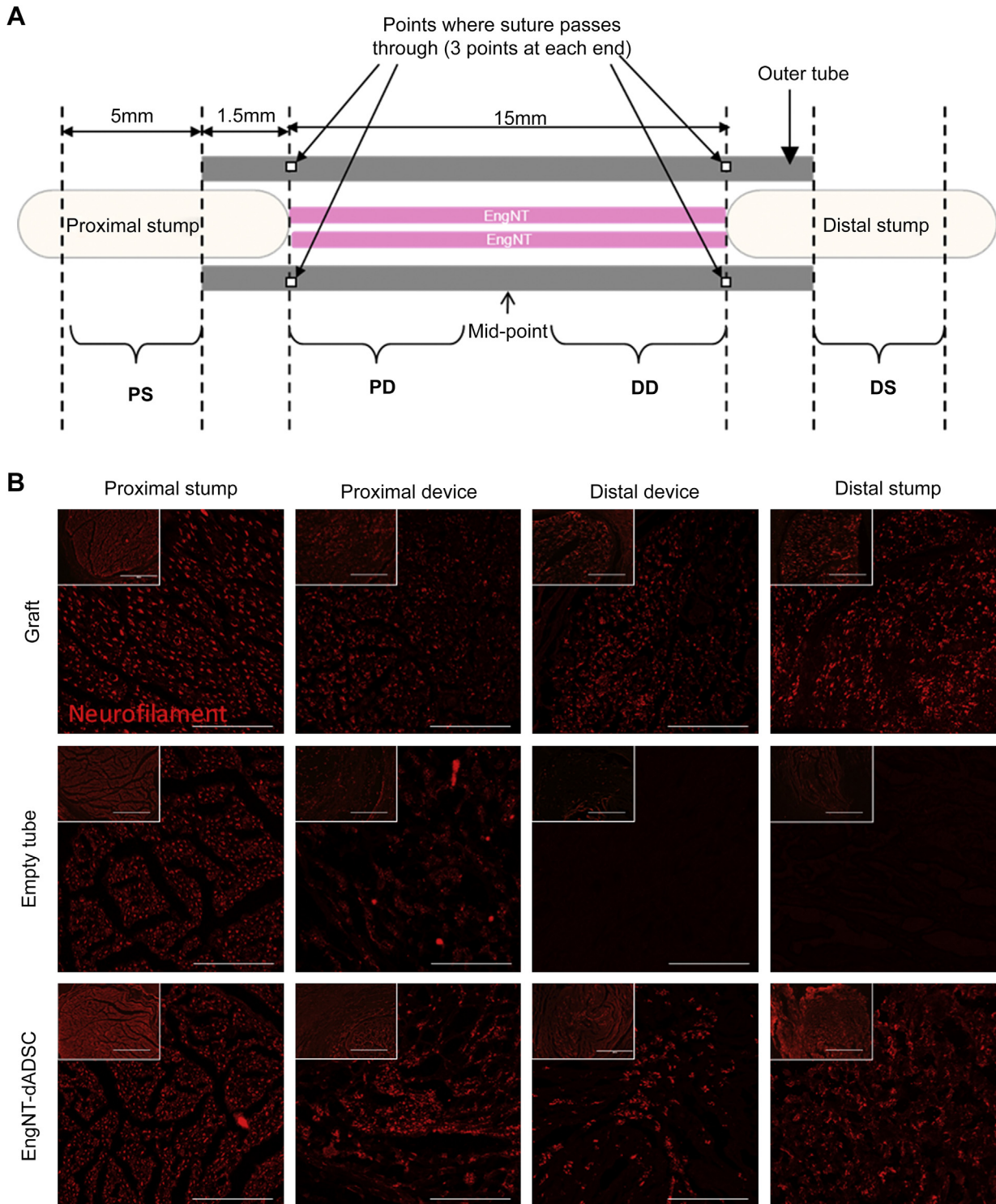
Fig. 5. EngNT-dADSC supports regeneration through a 15 mm repair device and into the distal stump. (A) Transverse sections were taken at four different positions within the repair site; the proximal stump (PS), proximal device (PD), distal device (DD) and distal stump (DS). (B) Micrographs show neurofilament antibody staining used to detect regenerating axons in the graft, empty tube and EngNT-dADSC (scale bars 100 μm). Insets show lower magnification views of the cross sections (scale bars 200 μm).

to show that the regenerating front detected by MRI was significantly longer in rats treated with dADSCs compared with an empty tube control [43].

The majority of the studies investigating the effects of dADSCs on nerve regeneration have utilised the 10 mm rat sciatic nerve injury model. There is little consensus about the most appropriate pre-clinical model to use for testing peripheral nerve repair devices

[44], so in this study we chose a relatively long gap (15 mm) and short time point (8 weeks) in the rat sciatic nerve which we know from our previous studies is a critical sized defect that shows poor regeneration when empty tubes are used, as reflects the long-gap situation in humans [10]. There are numerous possible methods for delivering EngNT to the site of nerve injury and further optimisation of the assembly and organisation of EngNT sheets into
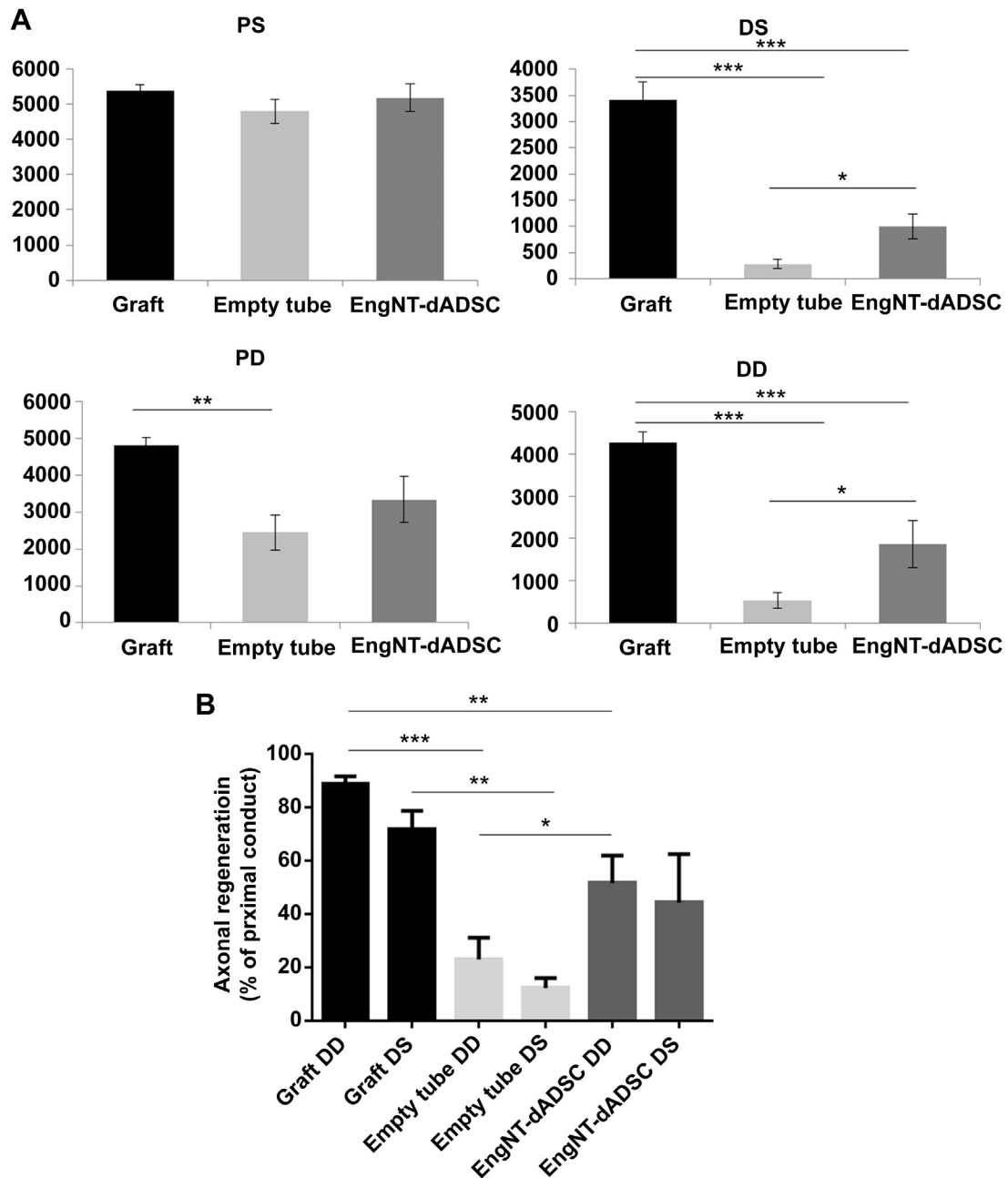
Fig. 6. Quantification of regeneration through the grafts and repair devices. (A) The ability of the repairs to support regeneration through the device and into the distal stump was assessed by counting the number of neurofilament positive axons (y axis) at the four different positions through the repairs, proximal stump (PS), proximal device (PD), distal device (DD) and distal stump (DS). Data are means ± SEM showing the number of axons in each repair at the different positions. (B) The ability of each repair to support neuronal growth was assessed by comparing the number of axons detected at the proximal part of the conduit to those detected at the distal end and in the distal stump. Data are means ± SEM. $^*P < 0.05$, $^{**}P < 0.01$, $^{***}P < 0.001$, repeated measures ANOVA with Tukey's post-test.

constructs as well as optimising the number of constructs will be the subject of future investigations. For the purposes of this work, EngNT-dADSC sheets were rolled to form rods of 15 mm length × 200 μm diameter and two of them were implanted within each NeuraWrap sheath as described previously [10]. This approach of rolling the EngNT sheets to form rods enabled them to be handled easily so they could be positioned between the nerve stumps, providing a continuous column of aligned dADSCs across the repair site.

Analysis of the mid-point of the repair site after 8 weeks revealed that there was considerably more regenerated neural tissue present in the EngNT-dADSC repairs compared to the empty

tube control group. Ultrastructural examination showed that the pattern of myelinated and unmyelinated nerve fibres present in the EngNT-dADSC repairs resembled that in the nerve graft controls, whereas regeneration in the empty tubes was sparse. There were no significant differences in nerve fibre diameter, axon diameter and G ratio between any of the groups, although myelin thickness was significantly reduced in the empty tube controls. As reported previously with EngNT-Schwann cells in the same model, this indicates that the quality of regeneration is similar in all groups and the main difference between them is the overall amount of regeneration [10]. From these experiments it is not possible to determine whether the dADSCs themselves are responsible for

myelinating the regenerating axons or if they enhance the myelination by the endogenous Schwann cells. However, *in vitro* studies have shown that dADSCs can form myelin whereas undifferentiated ADSC do not [45]. There is also some immunohistochemical evidence that transplanted dADSC actively contribute to the formation of myelin sheaths in a chronically denervated rat common peroneal nerve model [24].

To investigate the ability of EngNT-dADSC to support neuronal growth from the proximal to the distal stump, analyses were carried out to assess the number of regenerating neurites at different points across the repair site. Approximately 50% of the axons regenerated across the 15 mm inter-stump gap from the proximal to distal part of the device, and approximately 44% of the axons in the proximal part of the device traversed the gap and entered the distal stump. In contrast, only 12% of the axons in the proximal end regenerated through the empty conduit and into the distal stump. Previous studies have shown that ADSCs can support regeneration across short gaps. dADSCs transplanted in fibrin nerve conduits to treat a 10 mm sciatic nerve defect were shown to enhance the number of regenerating motor neurons, improve electrophysiological outcomes and increase distal axon myelination [21]. In another study, trans-differentiated ADSCs were combined with decellularised artery grafts to treat a rat facial nerve lesion [46]. The transplanted cells maintained their Schwann cell-like phenotype and myelin forming capabilities and long term morphological and functional evaluations showed that these cells were as effective as Schwann cells [46]. Manipulation of ADSCs by alternative differentiation protocols has also been shown to generate cells with enhanced regenerative capabilities for peripheral nerve repair [23,32,47]. As far as we are aware only one other study has utilised ADSCs in the 15 mm rat sciatic nerve gap model [48]. In that study, Schwann cell-like ADSCs were used to supplement acellular nerve grafts and the combined grafts showed positive effects on nerve regeneration and some enhancements in functional recovery compared with the acellular grafts [48].

5. Conclusions

Our results show that the EngNT-dADSC can be used to form an effective peripheral nerve repair device to bridge a critical sized nerve gap. Adipose-derived stem cells are an ideal candidate for a neural cell therapy because they are easily accessible from the patient for use in an autologous cell therapy, eliminating the risk of rejection from the patient, and they can be expanded in a controlled and reproducible manner. The dADSCs show phenotypic characteristics of Schwann cells and secrete a plethora of growth factors important for peripheral nerve regeneration. Importantly, the regenerative phenotype of dADSCs is enhanced in EngNT, both in terms of expression of neurotrophic and angiogenic factors and in terms of morphology and organisation. This is therefore a potentially powerful approach for delivering these cells within a peripheral nerve repair conduit. Enhancing the pro-regenerative phenotype of dADSCs while simultaneously organising the cells into aligned columns within a stable aligned collagen matrix provides a convenient means to assemble an artificial repair tissue. Furthermore, delivering dADSCs via stable EngNT constructs provides a way to distribute and organise the therapeutic cells within the nerve repair environment, offering a level of control that is not possible when cells are delivered in suspension or within disorganised unstable hydrogels. Future work will focus on optimisation of EngNT-dADSC to enhance further the pro-regenerative phenotype of the cells and determine the most effective way to organise the material to promote regeneration that leads to improvements in recovery of function *in vivo*. It will also be important to explore the use of human ADSCs in EngNT in order to develop this potentially beneficial combination of technologies towards the clinic.

Appendix A. Supplementary data

Supplementary data related to this article can be found at http://dx.doi.org/10.1016/j.biomaterials.2014.10.009.

References

[1] Ruijs AC, Jaquet JB, Kalmijn S, Giele H, Hovius SE. Median and ulnar nerve injuries: a meta-analysis of predictors of motor and sensory recovery after modern microsurgical nerve repair. Plast Reconstr Surg 2005;116:484—94. discussion 95-6.

[2] Ichihara S, Inada Y, Nakamura T. Artificial nerve tubes and their application for repair of peripheral nerve injury: an update of current concepts. Injury 2008;39(Suppl. 4):29—39.

[3] Kehoe S, Zhang XF, Boyd D. FDA approved guidance conduits and wraps for peripheral nerve injury: a review of materials and efficacy. Injury 2012;43: 553—72.

[4] Daly W, Yao L, Zeugolis D, Windebank A, Pandit A. A biomaterials approach to peripheral nerve regeneration: bridging the peripheral nerve gap and enhancing functional recovery. J R Soc Interface 2012;9:202—21.

[5] Bellamkonda RV. Peripheral nerve regeneration: an opinion on channels, scaffolds and anisotropy. Biomaterials 2006;27:3515—8.

[6] Gu X, Ding F, Yang Y, Liu J. Construction of tissue engineered nerve grafts and their application in peripheral nerve regeneration. Prog Neurobiol 2011;93: 204—30.

[7] Rodrigues MC, Rodrigues Jr AA, Glover LE, Voltarelli J, Borlongan CV. Peripheral nerve repair with cultured Schwann cells: getting closer to the clinics. ScientificWorldJournal 2012;2012:413091.

[8] Gupta D, Venugopal J, Prabhakaran MP, Dev VR, Low S, Choon AT, et al. Aligned and random nanofibrous substrate for the in vitro culture of Schwann cells for neural tissue engineering. Acta Biomater 2009;5:2560—9.

[9] Wang X, Luo E, Li Y, Hu J. Schwann-like mesenchymal stem cells within vein graft facilitate facial nerve regeneration and remyelination. Brain Res 2011;1383:71—80.

[10] Georgiou M, Bunting SC, Davies HA, Loughlin AJ, Golding JP, Phillips JB. Engineered neural tissue for peripheral nerve repair. Biomaterials 2013;34: 7335—43.

[11] Phillips JB. Building stable anisotropic tissues using cellular collagen gels. Organogenesis 2014;10:6—8.

[12] Guest JD, Rao A, Olson L, Bunge MB, Bunge RP. The ability of human Schwann cell grafts to promote regeneration in the transected nude rat spinal cord. Exp Neurol 1997;148:502—22.

[13] Walsh S, Midha R. Use of stem cells to augment nerve injury repair. Neurosurgery 2009;65:A80—6.

[14] Mosahebi A, Fuller P, Wiberg M, Terenghi G. Effect of allogeneic Schwann cell transplantation on peripheral nerve regeneration. Exp Neurol 2002;173: 213—23.

[15] Fraser JK, Wulur I, Alfonso Z, Hedrick MH. Fat tissue: an underappreciated source of stem cells for biotechnology. Trends Biotechnol 2006;24:150—4.

[16] D'Ippolito G, Schiller PC, Ricordi C, Roos BA, Howard GA. Age-related osteogenic potential of mesenchymal stromal stem cells from human vertebral bone marrow. J Bone Miner Res 1999;14:1115—22.

[17] Jiang L, Zhu JK, Liu XL, Xiang P, Hu J, Yu WH. Differentiation of rat adipose tissue-derived stem cells into Schwann-like cells in vitro. Neuroreport 2008;19:1015—9.

[18] Kaewkhaw R, Scutt AM, Haycock JW. Anatomical site influences the differentiation of adipose-derived stem cells for Schwann-cell phenotype and function. Glia 2011;59:734—49.

[19] Kingham PJ, Kalbermatten DF, Mahay D, Armstrong SJ, Wiberg M, Terenghi G. Adipose-derived stem cells differentiate into a Schwann cell phenotype and promote neurite outgrowth in vitro. Exp Neurol 2007;207:267—74.

[20] Radtke C, Schmitz B, Spies M, Kocsis JD, Vogt PM. Peripheral glial cell differentiation from neurospheres derived from adipose mesenchymal stem cells. Int J Dev Neurosci 2009;27:817—23.

[21] di Summa PG, Kalbermatten DF, Pralong E, Raffoul W, Kingham PJ, Terenghi G. Long-term in vivo regeneration of peripheral nerves through bioengineered nerve grafts. Neuroscience 2011;181:278—91.

[22] di Summa PG, Kingham PJ, Raffoul W, Wiberg M, Terenghi G, Kalbermatten DF. Adipose-derived stem cells enhance peripheral nerve regeneration. JPlastReconstrAesthetSurg 2010;63:1544—52.

[23] Gu JH, Ji YH, Dhong ES, Kim DH, Yoon ES. Transplantation of adipose derived stem cells for peripheral nerve regeneration in sciatic nerve defects of the rat. Curr Stem Cell Res Ther 2012;7:347—55.

[24] Tomita K, Madura T, Mantovani C, Terenghi G. Differentiated adipose-derived stem cells promote myelination and enhance functional recovery in a rat model of chronic denervation. J Neurosci Res 2012;90:1392—402.

[25] Widgerow AD, Salibian AA, Lalezari S, Evans GR. Neuromodulatory nerve regeneration: adipose tissue-derived stem cells and neurotrophic mediation in peripheral nerve regeneration. J Neurosci Res 2013;91:1517—24.

[26] Kolar MK, Kingham PJ. Regenerative effects of adipose-tissue-derived stem cells for treatment of peripheral nerve injuries. Biochem Soc Trans 2014;42: 697—701.

[27] Marconi S, Castiglione G, Turano E, Bissolotti G, Angiari S, Farinazzo A, et al. Human adipose-derived mesenchymal stem cells systemically injected promote peripheral nerve regeneration in the mouse model of sciatic crush. Tissue Eng Part A 2012;18:1264—72.

[28] Reid AJ, Sun M, Wiberg M, Downes S, Terenghi G, Kingham PJ. Nerve repair with adipose-derived stem cells protects dorsal root ganglia neurons from apoptosis. Neuroscience 2011;199:515—22.

[29] Kingham PJ, Kolar MK, Novikova LN, Novikov LN, Wiberg M. Stimulating the neurotrophic and angiogenic properties of human adipose-derived stem cells enhances nerve repair. Stem Cells Dev 2014;23:741—54.

[30] Tomita K, Madura T, Sakai Y, Yano K, Terenghi G, Hosokawa K. Glial differentiation of human adipose-derived stem cells: implications for cell-based transplantation therapy. Neuroscience 2013;236:55—65.

[31] Scholz T, Sumarto A, Krichevsky A, Evans GR. Neuronal differentiation of human adipose tissue-derived stem cells for peripheral nerve regeneration in vivo. Arch Surg 2011;146:666—74.

[32] Zhang Y, Luo H, Zhang Z, Lu Y, Huang X, Yang L, et al. A nerve graft constructed with xenogeneic acellular nerve matrix and autologous adipose-derived mesenchymal stem cells. Biomaterials 2010;31:5312—24.

[33] Brown RA, Wiseman M, Chuo CB, Cheema U, Nazhat SN. Ultrarapid engineering of biomimetic materials and tissues: Fabrication of nano- and microstructures by plastic compression. Adv Funct Mater 2005;15:1762—70.

[34] East E, Golding JP, Phillips JB. A versatile 3D culture model facilitates monitoring of astrocytes undergoing reactive gliosis. J Tissue Eng Regen Med 2009;3:634—46.

[35] Wright KE, Liniker E, Loizidou M, Moore C, Macrobert AJ, Phillips JB. Peripheral neural cell sensitivity to mTHPC-mediated photodynamic therapy in a 3D in vitro model. Br J Cancer 2009;101:658—65.

[36] di Summa PG, Kalbermatten DF, Raffoul W, Terenghi G, Kingham PJ. Extracellular matrix molecules enhance the neurotrophic effect of Schwann cell-like differentiated adipose-derived stem cells and increase cell survival under stress conditions. Tissue Eng Part A 2013;19:368—79.

[37] Ribeiro-Resende VT, Koenig B, Nichterwitz S, Oberhoffner S, Schlosshauer B. Strategies for inducing the formation of bands of Bungner in peripheral nerve regeneration. Biomaterials 2009;30:5251—9.

[38] Martens W, Sanen K, Georgiou M, Struys T, Bronckaers A, Ameloot M, et al. Human dental pulp stem cells can differentiate into Schwann cells and promote and guide neurite outgrowth in an aligned tissue-engineered collagen construct in vitro. FASEB J 2014;28:1634—43.

[39] Richardson JA, Rementer CW, Bruder JM, Hoffman-Kim D. Guidance of dorsal root ganglion neurites and Schwann cells by isolated Schwann cell topography on poly(dimethyl siloxane) conduits and films. J Neural Eng 2011;8: 046015.

[40] Seggio AM, Narayanaswamy A, Roysam B, Thompson DM. Self-aligned Schwann cell monolayers demonstrate an inherent ability to direct neurite outgrowth. J Neural Eng 2010;7:046001.

[41] Thompson DM, Buettner HM. Neurite outgrowth is directed by schwann cell alignment in the absence of other guidance cues. Ann Biomed Eng 2006;34: 161—8.

[42] Lopatina T, Kalinina N, Karagyaur M, Stambolsky D, Rubina K, Revischin A, et al. Adipose-derived stem cells stimulate regeneration of peripheral nerves: BDNF secreted by these cells promotes nerve healing and axon growth de novo. PLoS One 2011;6:e17899.

[43] Tremp M, Meyer Zu SM, Kappos EA, Engels PE, Fischmann A, Scherberich A, et al. The regeneration potential after human and autologous stem cell transplantation in a rat sciatic nerve injury model can be monitored by MRI. Cell Transplant 2013. http://dx.doi.org/10.3727/096368913X676934.

[44] Angius D, Wang H, Spinner RJ, Gutierrez-Cotto Y, Yaszemski MJ, Windebank AJ. A systematic review of animal models used to study nerve regeneration in tissue-engineered scaffolds. Biomaterials 2012;33:8034—9.

[45] Wei Y, Gong K, Zheng Z, Liu L, Wang A, Zhang L, et al. Schwann-like cell differentiation of rat adipose-derived stem cells by indirect co-culture with Schwann cells in vitro. Cell Prolif 2010;43:606—16.

[46] Sun F, Zhou K, Mi WJ, Qiu JH. Repair of facial nerve defects with decellularized artery allografts containing autologous adipose-derived stem cells in a rat model. Neurosci Lett 2011;499:104—8.

[47] Hsueh YY, Chang YJ, Huang TC, Fan SC, Wang DH, Chen JJ, et al. Functional recoveries of sciatic nerve regeneration by combining chitosan-coated conduit and neurosphere cells induced from adipose-derived stem cells. Biomaterials 2014;35:2234—44.

[48] Wang Y, Zhao Z, Ren Z, Zhao B, Zhang L, Chen J, et al. Recellularized nerve allografts with differentiated mesenchymal stem cells promote peripheral nerve regeneration. Neurosci Lett 2012;514:96—101.